J Mater Sci (2010) 45:2023–2029
DOI 10.1007/s10853-009-3946-1

HTC2009

A study on the interfacial tension between solid iron and CaO–SiO_2–MO system

**Eun-Jin Jung · Wook Kim · Il Sohn ·
Dong-Joon Min**

Received: 15 June 2009 / Accepted: 2 October 2009 / Published online: 15 October 2009

Abstract Interfacial tension is an important property that plays an essential role in understanding wetting behavior between refractories–molten slag–steel in the steelmaking process. Most work on interfacial tensions of molten slag system have been done to clarify the effect of surface active elements in molten metal and slag composition, but there has been little work done with respect to the slags ionic structure. In this study, the interfacial tension between molten slag and solid Fe was investigated to understand the effect of the ionic structure of molten slag on interfacial tension by using solid Fe instead of molten steel. Interfacial tension measurements in CaO–SiO_2–FeO and CaO–SiO_2–MnO slags were carried out at 1,773 K on interstitial free (IF)-steel substrates using the sessile drop method. The composition of the slag was varied with amphoteric oxides of either FeO or MnO at unit basicity ($C/S = 1.0$). Results indicated a decrease in the interfacial tension with increased amphoteric oxide additions. The ionic species of molten slags were analyzed by FT-IR and the various types of oxygen ions (O^{2-}, O^{-}, $O^{0)}$ in the slag was determined by X-ray photoelectron spectroscopy. The silicate bonding degree and the slags ionic behavior were semi-quantitatively analyzed with respect to the slag's ionic structure model. By dissociating the slags networking structure with increased free oxygen ions, the interfacial tension decreased. Considering the ionic theory of molten slags, results indicate that the interfacial properties are directly affected by the ionic structure of the slag. This work hopes to clarify the relationship between the interfacial tension and the distribution of various oxygen ions.

Introduction

Slag in ironmaking and steelmaking processes has been utilized to prevent the contamination of molten steel from the atmosphere, to provide thermal insulation, and to remove impurities in molten steel. Slag as mixture of oxide has specific properties of melting temperature, low viscosity, and low surface/interfacial tension quite different from molten iron. Optimal slag properties require low thermal conductivity for better thermal insulation, low diffusion coefficients to inhibit unwanted pickup from the atmosphere and increased absorption capacity for non-metallic inclusion removal. Physicochemical properties of slag and molten metal directly affect the surface and interfacial properties in the refining process of molten metal. Interfacial tension, which is one of the basic properties of molten slag, not only determines the slag fluidity and subsequently the substance migration in the refining process, but also the wettability between coke/refractory/slag in the iron and steelmaking processes. Beyond the steelmaking processes, this property also plays an important role in the insulation efficiency of the flux in a welding process. Interfacial reactions between two phases affect the interfacial tension, which can significantly impact specific steelmaking processes details of which has been published elsewhere [1–5].

Interfacial energy is a strong correlation between the solid and liquids with certain bulk properties, which

---

E.-J. Jung · W. Kim · I. Sohn · D.-J. Min (✉)
Department of Materials Science and Engineering,
Yonsei University, Seoul 120-749, Korea
e-mail: chemical@yonsei.ac.kr

E.-J. Jung
e-mail: design-82@hanmail.net

W. Kim
e-mail: knight62@hanmail.net

I. Sohn
e-mail: ilsohn@yonsei.ac.kr

depend directly in the interatomic potential. This atomic mismatch results in interfacial tension (γ), and can be derived by measuring the contact angle (θ) using Young's equation [6] given below:

$$\gamma_{\mathrm{M/G}} = \cos\theta \cdot \gamma_{\mathrm{S/G}} + \gamma_{\mathrm{M/S}}, \qquad (1)$$

where $\gamma_{\mathrm{S/G}}$ and $\gamma_{\mathrm{M/G}}$ are the surface tension of the slag and the metal phase, respectively. $\gamma_{\mathrm{M/S}}$ is the interfacial tension between the solid metal and the liquid slag. This equation can also be derived by minimizing free energy and a number of detailed derivations are available [7, 8].

Pioneering work by Gibbs adsorption isotherm [9] on interfacial tension measurements focused on the effect of surface/interfacial active elements such as O and S at very low concentration in liquid Fe [10–12]:

$$\Gamma = -\frac{1}{\mathrm{RT}} \cdot \frac{\mathrm{d}\gamma}{\mathrm{d}\ln a_{\mathrm{O}}}, \qquad (2)$$

where γ is the surface tension, Γ is the saturation coverage, and a_{o} the activity of oxygen in liquid Fe. Using the Gibbs adsorption isotherm and the Gibbs–Belton equation, Mori and coworkers [11] and Cramb and Jimbo [12] investigated the influence of oxygen in molten metal (a_{o}) according to the slag composition. However, these studies of interfacial tension with liquid Fe are complicated by the equilibrium oxygen concentration between liquid Fe/slag and the ionic structural effect of molten slag. Thus, to minimize this effect of oxygen in molten Fe by interaction with slag, a solid Fe substrate should be introduced.

Tanaka and coworkers [13, 14] modified Bulter's result considering the effect of ionic radius ratio ($R_{\mathrm{cation}}/R_{\mathrm{anion}}$) for the surface tension of molten ionic mixtures. However, the correlation between the interfacial tension and the slag structure was still unclear.

Therefore, in the present study, the relationship between the interfacial tension and the ionic structure of slag was investigated with particular emphasis on the ionic structure of slag at the interface of the CaO–SiO_2–FeO and CaO–SiO_2–MnO slag system and the behavior of amphoteric oxides of FeO and MnO in the slag by Fourier transform infrared spectroscopy (FT-IR). In addition, the effect of the various ionic oxygen species at the interface with variation in slag composition is also discussed using X-ray photoelectron spectroscopy (XPS).

Experimental

Reagent-grade chemicals of SiO_2, MnO, FeO, and $CaCO_3$ were used to produce the appropriate slag composition. Interstitial free (IF) steels were used to provide ultra clean steel for simulation of a pure Fe substrate. The chemical composition of the IF steel (solid Fe substrate) is given in Table 1. To measure the contact angle of the slag with the solid Fe substrate, 10 g of the mixed powder was premelted in a molybdenum crucible. The premelted slag sample was quenched in water-cooled copper plate. The master slag was analyzed using an X-ray fluorescence (XRF, Bruker-S4 Explorer) Spectrometer. 1.3 g of the master slags was pressed into cylindrical tablets of 13 mm diameter for contact angle measurements. To evaluate the effect of only slag structure on interfacial tension, and minimize the impact of surface active element at the slag/metal interface, the interfacial tension between molten slag and solid Fe. Thus, the interfacial tension between molten slag and solid Fe can be reasonably assumed to be controlled only by the slag structure and the behavior of various types of oxygen ions at the interface. Furthermore, to minimizing the side effect of the surface roughness of solid Fe, the surface was polished up to 50 nm with α-Al_2O_3 powder. The contact angle was measured by melting the slag in a horizontal furnace at 1,773 K and taking multiple frames every 10 s of the slag/metal interface with a telephotographic camera (Canon, EOS 350D). Using the contact angle, the interfacial tension was obtained by Young's equation. Figure 1 shows the schematic diagram of the experimental device for contact angle measurements. The horizontal mullite tube was initially flushed with Ar gas (200 sccm) up to the target temperature and switched to 95% Ar/5% H_2 gas mixture (200 sccm) to prevent the oxidation of Fe substrate. The slag samples were quenched, crushed, and sieved below 100 µm for Fourier transform infrared spectroscopy (FT-IR, PerkinElmer-spectrum 100) analysis to semi-quantitatively identify the structure of the slag. Also, the surface of the slag at the slag/metal interface was analyzed after separating the slag from the Fe substrate using an X-ray photoelectron spectroscopy (XPS, Sigma Probe-ThermoVG) with a monochromatic Al-Kα source (15 kV, 100 W, 400 µm) and a C_{1s} spectra(285 eV) for the calibration standard. These slags were measured using a ThermoVG with a chamber pressure maintained below 7×10^{-9} hPa during acquisition.

Table 1 Composition of IF steel (wt%)

Subject	C	Mn	Si	Cr	Ti	N	O
Content	0.007	0.53	0.00	0.06	0.02	0.001	0.004

Results and discussion

Interfacial tension

As previously mentioned, the interfacial tension can be determined by measuring the contact angle and Young's

Fig. 1 Schematic diagram for measurement of contact angle

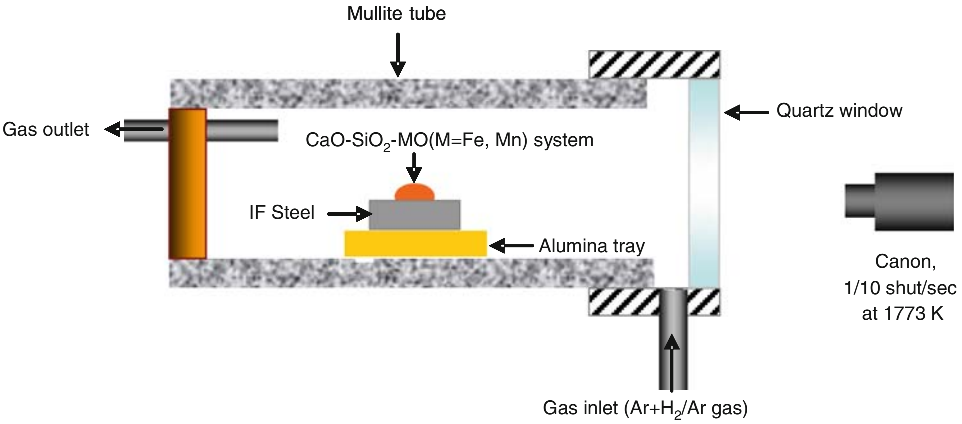

Fig. 2 Measurement of the contact angle to derive interfacial tension using Young's equation

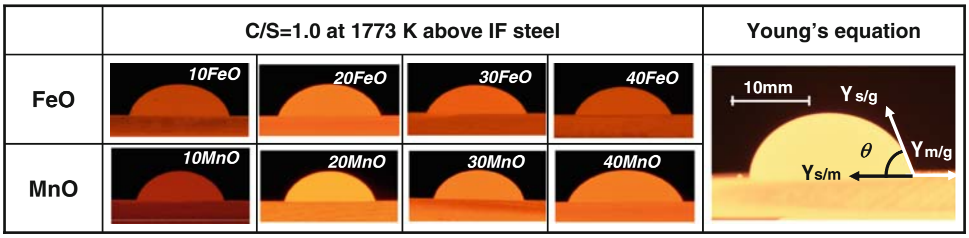

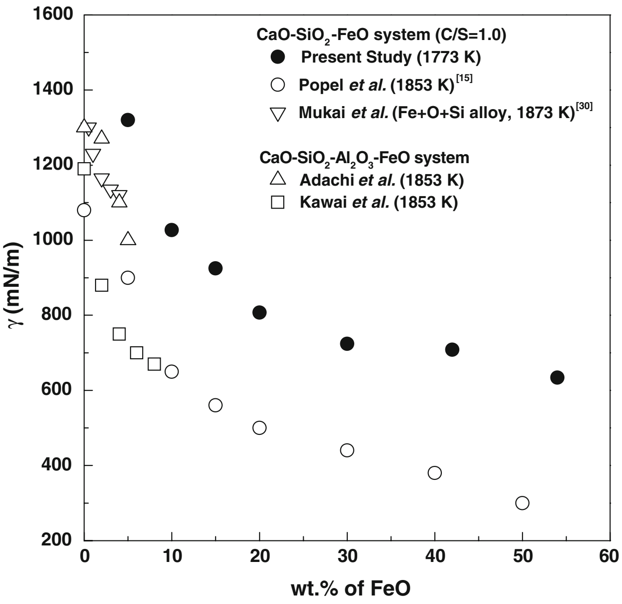

Fig. 3 Effect of FeO in slag on the interfacial tension between iron and slag

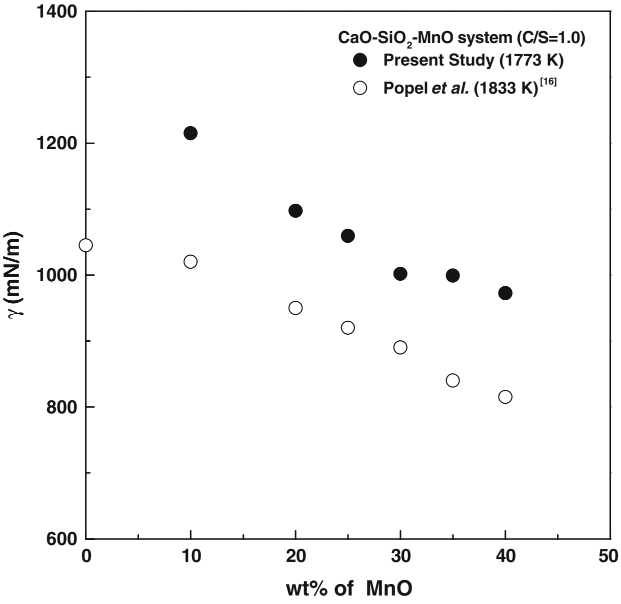

Fig. 4 Effect of MnO in slag on the interfacial tension between iron and slag

equation. Typical contact angle measured in the present study is shown Fig. 2. The change in the interfacial tension with additions of FeO and MnO under unit basicity ($C/S = 1.0$) is discussed. Figures 3 and 4 shows that the interfacial tension decreases with the addition of FeO and MnO. Although Popel et al. [15, 16] performed similar measurements for the indicated slag system, the Fe state used by Popel et al. was liquid phase, and the interfacial tension was 200 mN/m lower than the results of this study using a solid Fe substrate. The discrepancy with Popel et al. would be expected due to the relatively loose bonding of the Fe in the liquid state and its increased readiness for reaction with slag ions.

Present experimental results simply represent the degree of dissociation of silicates in the slag structure with the additions of FeO and MnO by using FT-IR. FT-IR can be used to qualitatively estimate the degree of the silicate network structure dissociation and XPS can be used to correlate between the interfacial tension and ionic oxygen states through the change in the ions of the slag located at the slag/Fe substrate interface.

Structure of molten slag

Based on the results of this experiment, changes in the structure of the slag were investigated using FT-IR. Figure 5 shows the results of the FT-IR analysis. In general, the analysis based on the slag structure can be considered as an analysis that represents the change of silicate anion groups according to the addition of free oxygen ions, which are dissociated from the following basic oxides [17]. The dissociation of slag structure based on silicate anion groups is represented NBO/Si (non-bridging oxygen per silicon). It is described by the following equations:

$$\mathrm{MO} = \mathrm{M}^{2+} + \mathrm{O}^{2-}, \tag{3}$$

$$[\mathrm{Si_3O_9}]^{6-}(\mathrm{ring}) + \mathrm{O}^{2-} = [\mathrm{Si_3O_{10}}]^{8-}(\mathrm{chain}), \tag{4}$$

$$[\mathrm{Si_3O_{10}}]^{8-}(\mathrm{chain}) + \mathrm{O}^{2-} = [\mathrm{Si_2O_7}]^{6-}(\mathrm{dimer}) + [\mathrm{SiO_4}]^{4-}(\mathrm{monomer})\,, \tag{5}$$

$$3[\mathrm{Si_2O_7}]^{6-} = 2[\mathrm{SiO_3}]^{2-} + 2[\mathrm{SiO_4}]^{4-}, \tag{6}$$

where M^{2+} represents the metallic cations, such as Ca^{2+}, Mg^{2+}, Fe^{2+}, and Mn^{2+}. The slag network structure can be dissociated by generating $[\mathrm{Si_2O_7}]^{6-}$-dimers (NBO/Si = 3) and $[\mathrm{SiO_4}]^{4-}$-tetrahedra (NBO/Si = 4), which are the silicate unit cell simplified by the reactions of (4) and (5), that occur spontaneously with the supply of free oxygen ion. Also, each silicate anion group is separated by increasing the NBO/Si and indicates simplification or depolymerization of the slag structure. Thus the silicate unit in slag exists as a relatively small sized flow unit and it is possible to correlate between the interfacial tension and the flow unit by investigating the structure of slag using an FT-IR.

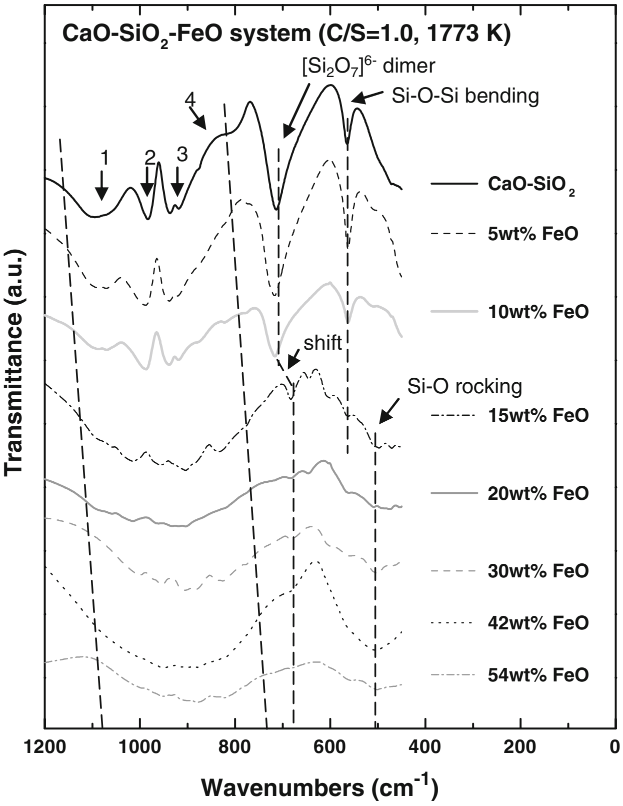

Fig. 5 FT-IR spectrometric analysis of CaO–SiO$_2$–FeO system

Figure 5 showed result of the FT-IR for the CaO–SiO$_2$–FeO system as a function of its composition and wave number. From the aforementioned existing studies on similar slag systems [18], the four major IR bands that correspond to $[\mathrm{SiO_4}]^{4-}$-tetrahedra can be observed at about 1,060, 975, 905, and 860 cm^{-1}, respectively. The NBO for each band corresponds to the waver number of 1, 2, 3, and 4. In addition the $[\mathrm{Si_2O_7}]^{6-}$-dimers exist at about 705 cm^{-1}, the [Si–O–Si]-bending is at about 570 cm^{-1}, and the [Si–O]-rocking is at about 500 cm^{-1}. The NBO configured by 1, 2, and 3, $[\mathrm{Si_2O_7}]^{6-}$-dimers, and [Si–O–Si]-bending peak were present with no FeO addition. However, there was a small increase in transmittance ($\%T = (I/I_0) \times 100$) with additions of FeO below 15 wt% and also no significant shifts in peaks. It should be noted that the dissociation of the slag structure correspond to increases in the FT-IR transmittance. However, the $[\mathrm{Si_2O_7}]^{6-}$-dimers and [Si–O–Si]-bending peak were not observed in the range of 20–54 wt% FeO. Also, the dimer peaks gradually disappeared as it shifted to lower frequencies.

This shift of the dimer peaks to the lower wave numbers indicates the dissociation of dimers and the decrease of the silicate attraction forces by amphoteric oxides. With increased dissociation of the dimer in the slag, the non-bridging oxygen ion (O^{-}) is produced in the monomer increasing the change density and resulting in a weaker structure [19]. In addition, the [Si–O]-rocking peak is observed above 15 wt% FeO. A rocking structure indicates a low binding force and exists at the lower section of the wave number than that of the NBO/Si, dimers, and bending peaks. This suggests that the silicate bond showed a more loose state than before [20]. Also, the center of gravity at about 1,100–900 cm^{-1} was slightly shifted to about 1,000–820 cm^{-1}, which indicates decrease in the degree of polymerization due to the increase in the chemical potential of free oxygen ion (O^{2-}) [21]. Therefore, considering the change in the silicate structure of the slag through FT-IR analysis, the gradient change of the interfacial tension was from the 20 wt% FeO correlation to the production of [Si–O]-rocking. In addition, the binding force decreased with the generation of $[\mathrm{SiO_4}]^{4-}$-monomers while the structure of the $[\mathrm{Si_2O_7}]^{6-}$-dimer in slag was dissociated. Figure 6 shows result of FT-IR

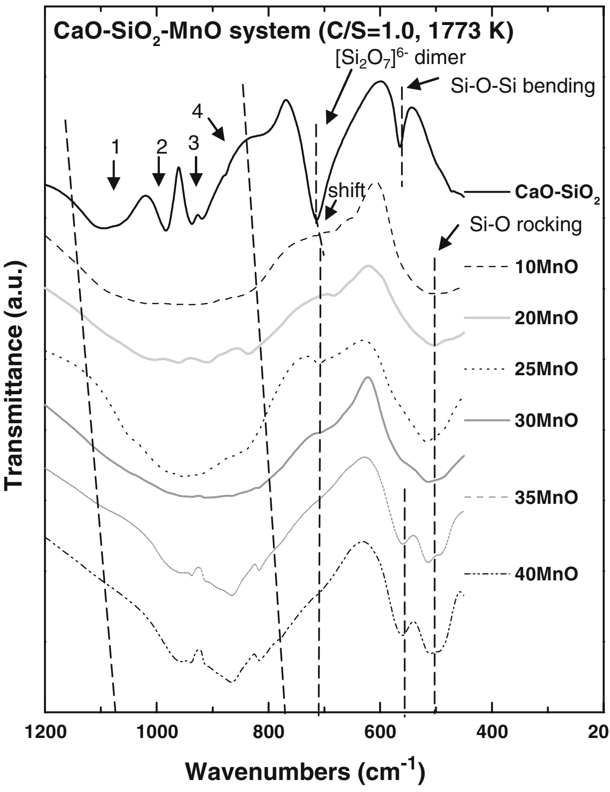

Fig. 6 FT-IR spectrometric analysis of CaO–SiO_2–MnO system

analysis for the CaO–SiO_2–MnO slag. Similar to FeO, the dissociated oxygen ions from the basic oxides break the silicates network structure into smaller dimmers and monomer units. The NBO of 1, 2, 3, the $[Si_2O_7]^{6-}$-dimer, and [Si–O-Si] bending peaks were clearly observed without MnO. With increased concentration of MnO, the various NBO/Si and the $[Si_2O_7]^{6-}$ disappeared due to the shift toward lower wave numbers. Also, the [Si–O–Si]-bending disappeared with MnO addition of up to 10% and replaced by the [Si–O]-rocking structure. The [Si–O–Si]-bending reappeared with 35% MnO and indicated relatively less dissociation of the silicate structure compared to FeO addition. The center of gravity was slightly shifted from 1,100–900 cm^{-1} to 1,000–820 cm^{-1}, which indicates the degree of polymerization decreased with increased chemical potential of O^{2-} ions. Thus, the $[Si_2O_7]^{6-}$-dimer structure of the slag dissociation decreases interaction forces between Si and O while a simple $[SiO_4]^{4-}$-monomer structure was generated.

Effect of oxygen ionic states at the interface

It is well known from electrical conductivity experiments [22, 23] that slags are indeed ionic. One of the earlier slag theories that sparked interest in slags ionic characteristic was developed by Temkin and coworkers [24] assuming complete dissociation of the slag solution and no interaction between ionic of the same charge. Using Temkin's model as a basis and the work done by Fincham and Richardson [25], where the oxygen ions in slag existed as free oxygen ion (O^{2-}), non-bridging oxygen ion (O^{-}), and bridging oxygen ion (O^{0}). Toop and Samis [26] further developed the ionic slag theory to determine the degree of polymerization of silicate anions in both acid and basic slags. Toop and Samis model is especially useful in estimating the fraction of the different oxygen ions existing in the slag. This was experimentally verified by Park et al. [27], where the effect of basicity on distribution of the three oxygen ion species in liquid slag using XPS. It was found to be reasonably comparable to the estimation obtained from Toop and Samis model.

Figure 7 shows the present results of the XPS analysis and the high-resolution spectra were fitted using Avantage (ThermoVG software package) with an accuracy of ±0.05 eV. According to Fig. 7, the ions of O^{-} and O^{2-} increased, and the O^{0} decreased at the interface between the Fe substrate and slag with addition of FeO. There is a slight deviation from Toop and Samis model and the XPS results in Fig. 7, which is expected considering the likelihood of relatively small slag ion interaction. Figure 8 shows the interfacial tension related to the O^{2-} based on the result of Fig. 7. The interfacial tension linearly decreases with increasing $\ln X_{O^{2-}}$. Although the basicity for the present study was fixed at 1.0, it is likely basicity influences the interfacial tension between molten slag and solid Fe.

Similar to the CaO–SiO_2–FeO system, Fig. 9 shows the results of the XPS analysis of the CaO–SiO_2–MnO slag

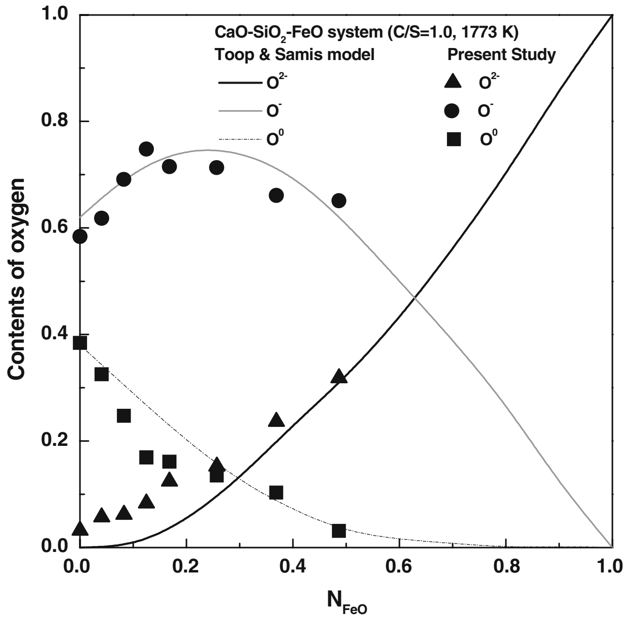

Fig. 7 Oxygens in CaO–SiO_2–FeO at 1,773 K by XPS

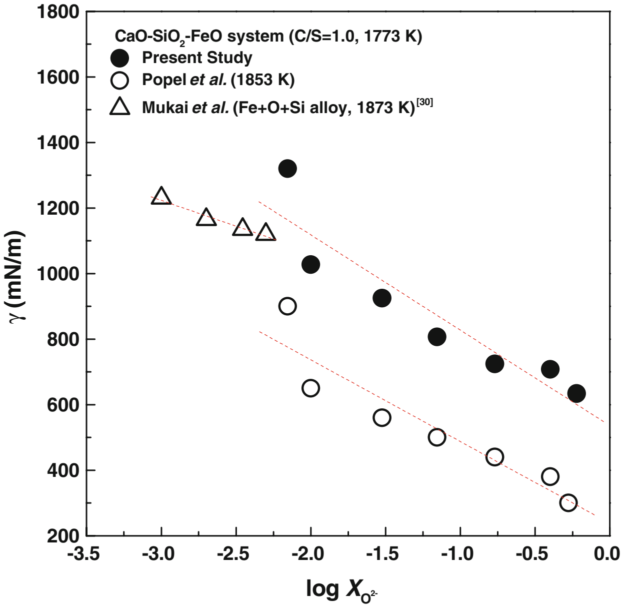

Fig. 8 Effect of oxygen content on interfacial tension between Fe and CaO–SiO_2–FeO slag system

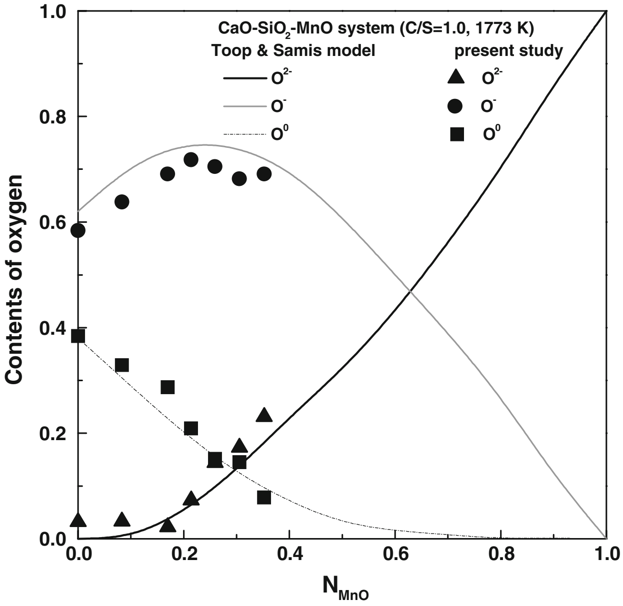

Fig. 9 Oxygens in CaO–SiO_2–MnO at 1,773 K by XPS

compared with Toop and Samis model. The oxygen concentration in the CaO–SiO_2–MnO system showed an increase in the amount of O^{2-} and O^- with MnO addition, but a decrease in the O^- ion above 0.2 mole of MnO similar to FeO. For O^{2-}, it continued to increase beyond 0.2 mole of MnO. This indicates the disappearance of the bonding oxygen while the structure of the silicate was dissociated. Thus, the decrease in the interfacial tension between solid Fe and molten slag is directly related to the increase in the ions of O^- and O^{2-}. If the effect of various oxygen species on interfacial tension is approached with respect to interface reaction sites, larger sized ions will affect interface properties more than smaller sized ions. According to Table 2 [28], the ionic radius of oxygen ions is larger than the cations. Thus, the oxygen species are expected to play a major role in interface properties. Furthermore, the Fe^{2+} non-bonding ion on the surface of the Fe substrate formed a reaction with the O^- or O^{2-} decreasing the contact angle.

The driving force of an interface between two materials is to decrease the free energy that occurs when intimate contact is established [29]. The interfacial tension significantly decreased with increased basicity in Fig. 10.

According to Figs. 8 and 10, interfacial tension is decreased with increasing content of free oxygen ion. Based on Gibbs adsorption isotherm of Eq. 2, interfacial tension and the activity of oxygen can be modified as follows.

$$\Gamma = -\frac{1}{\mathrm{RT}} \cdot \frac{\mathrm{d}\gamma}{\mathrm{d}\ln a_{\mathrm{O}^{2-}}} \approx -\frac{1}{\mathrm{RT}} \cdot \frac{\mathrm{d}\gamma}{\mathrm{d}\ln X_{\mathrm{O}^{2-}}}, \quad (7)$$

where $a_{O^{2-}}$ can be expressed as $X_{O^{2-}}$ if we assume complete dissociation and complete mixing resulting in a

Table 2 Ionic radius of cations and oxygen ion (Å) [28]

Elements	Si^{4+}	Ca^{2+}	Mn^{2+}	Na^+	O^{2-}	O^-	O^0
Radius (Å)	0.42	0.99	0.67	0.95	1.44	1.03	0.66

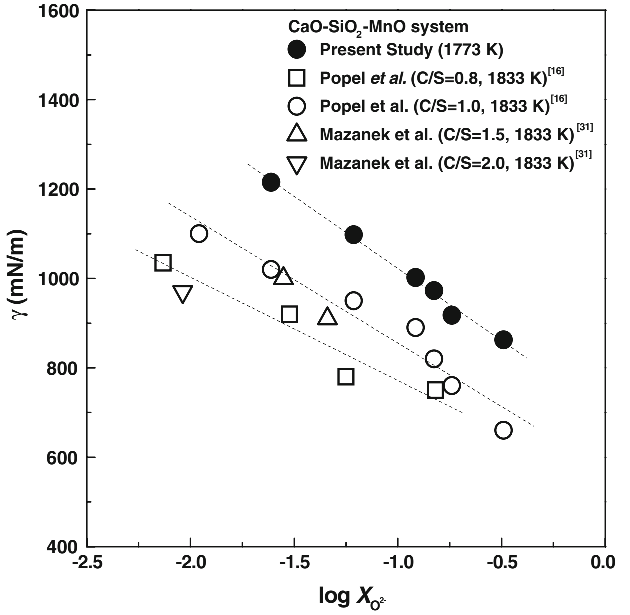

Fig. 10 Effect of oxygen content on interfacial tension between Fe and CaO–SiO_2–MnO slag system

constant activity coefficient similar to Toop and Samis model.

In Fig. 10, the slope of the interfacial tension with free oxygen ion was found to be approximately −0.533 and −0.647 for $C/S = 0.8$ and 1.0, respectively. Thus, Γ increased with higher basicity. And a linear relationship between the interfacial tension and $\ln X_{O^{2-}}$ was observed suggesting that the saturation coverage (Γ) is independent of slag concentration. Furthermore, the interfacial tension was more significantly affected by additions of FeO than MnO. The decrease in the interfacial tension with the addition of MnO and FeO was related to the attraction forces between Mn^{2+}/O^{2-} and Fe^{2+}/O^{2-} ion according to Coulombs law and silicate bonding force. Therefore, it is necessary to understand the interfacial tension with respect to the mole fraction of free oxygen ion and the addition of other constituents.

Conclusions

The interfacial tension of molten slag with solid Fe was studied using FT-IR and XPS. The results were focused on the slag structure of the $CaO–SiO_2–FeO$ and $CaO–SiO_2–MnO$ slag system. With increased oxygen ions, the dissociation of the slag network was verified. By controlling the slag composition using FeO and MnO at a constant unit basicity, the interfacial tension decreased with FeO and MnO additions. These findings can be applied to understanding and designing a slag with optimum interfacial properties to increase the refining and protective ability of novel slags.

(1) Changes in the interfacial tension was correlated with modifications in the slag structure when FeO is added. The structure of the slag was modified by adding the basic oxide FeO simplifying the silicate network structure.

(2) Three types of oxygen (free oxygen, non-bridging oxygen, bridging oxygen) in liquid slags were determined quantitatively. The interfacial tension linearly decreases with increasing $\ln X_{O^{2-}}$.

(3) MnO additions had relatively smaller dissociation in the silicate structure and thus less effect on the interfacial tension compared to FeO. The slope of the interfacial tension the $CaO–SiO_2–MnO$ slag as a function of $\ln X_{O^{2-}}$ was found to be about −0.533 and −0.647 for $C/S = 0.8$ and $C/S = 1.0$, respectively. For the $CaO–SiO_2–FeO$ system, the gradient was about −0.670 for $C/S = 1.0$.

Acknowledgements This work had been supported by 'Brain Korea 21 (BK 21) Project'. We gratefully appreciate additional financial support from the Division of Humantronics Information Materials (The YONSEI University of Seoul, Korea).

References

1. Sano N, Lu WK, Riboud PV (1997) Advanced physical chemistry for process metallurgy. Academics Press, San Diego, p 183
2. Sahajwalla V, Mehta AS, Khanna R (2004) Met Trans B 35B:75
3. Lee J, Kiyose A, Tanaka M, Tanaka T (2006) ISIJ Int 46(4):467
4. Nakashima K, Mori K (1992) ISIJ Int 32(1):11
5. Elliott JF (1985) Trans Inst Miner Metall C 94:171
6. Young T (1855) In: Peacock G (ed) Miscellaneous works, vol 1. John Murray, London
7. Howe JM (1993) Int Mater Rev 38:257
8. Ramqvist L (1965) Int J Powder Metall 1:2
9. Belton GR (1976) Met Trans B 7B:35
10. Ogino K, Hara S, Miwa T, Kimoto S (1984) Trans ISIJ 24:522
11. Sun H, Nakashima K, Mori K (2006) ISIJ Int 46(3):407
12. Cramb AW, Jimbo I (1989) Steel Res 60(3+4):157
13. Tanaka T, Kitamura T, Back IA (2006) ISIJ Int 46(3):400
14. Nakamoto M, Kiyose A, Tanaka T, Holappa L, Hamalainen M (2007) ISIJ Int 47(1):38
15. Popel SI (1958) Zh Fiz Khim 32(10):2398
16. Popel SI (1963) Sb Nauchn Tr Ural'sk Polit 126:5
17. De Kock RL, Gray HB (1989) Chemical structure and bonding. University Science Books, Mill Valley, p 419
18. Sridhar S, Mills KC, Afrange ODC, Lorz HP, Carli R (2000) Ironmak Steelmak 27:238
19. Dayanand C, Bhikshamaiah G, Tyagaraju VJ, Salagram M, Krishna Murthy ASR (1996) J Mater Sci 31:1945. doi:10.1007/BF00356615
20. Socrates G (1994) Infrared characteristic group frequencies, 2nd edn. Wiley, England
21. Park JH, Min DJ, Song HS (2006) ISIJ Int 42(4):344
22. Herasymenko P (1938) Trans Faraday Soc 34:1245
23. Downing LH, Urban L (1966) J Met 18:337
24. Samarin A, Temkin M, Schvartzman L (1945) Acta Physicochim 20:421
25. Fincham CJB, Richardson FD (1954) Proc R Soc 223:40
26. Toop GW, Samis CS (1962) Trans Met Soc AIME 224:878
27. Park JH, Rhee CH (2001) J Non-Cryst Solids 282:7
28. Shannon RD, Prewitt CT (1969) Acta Cryst B25:925
29. Howe JM (1997) Interfaces in materials. Wiley Interscience, New York, p 176
30. Mukai K, Furukawa H, Tsuchikawa T (1977) Tetsu-to-Hagane 50:1838
31. Mazanek T (1963) Arch Hutnictwa 8(2):119